Assembly Pathway of an AAA+ Protein: Tracking ClpA and ClpAP Complex Formation in Real Time†

Wolfgang Kress, Hannes Mutschler, and Eilika Weber-Ban*

Institute of Molecular Biology and Biophysics, ETH Zürich, 8093 Zürich, Switzerland

Received December 20, 2006; Revised Manuscript Received March 30, 2007

ABSTRACT: The ClpAP chaperone−protease complex is active as a cylindrically shaped oligomeric complex built of the proteolytic ClpP double ring as the core of the complex and two ClpA hexamers associating with the ends of the core cylinder. The ClpA chaperone belongs to the larger family of AAA$^+$ ATPases and is responsible for preparing protein substrates for degradation by ClpP. Here, we study in real time using fluorescence and light scattering stopped-flow methods the complete assembly pathway of this bacterial chaperone−protease complex consisting of ATP-induced ClpA hexamer formation and the subsequent association of ClpA hexamers with the ClpP core cylinder. We provide evidence that ClpA assembles into hexamers via a tetrameric intermediate and that hexamerization coincides with the appearance of ATPase activity. While ATP-induced oligomerization of ClpA is a prerequisite for binding of ClpA to ClpP, the kinetics of ClpA hexamer formation are not influenced by the presence of ClpP. Models for ClpA hexamerization and ClpA−ClpP association are presented along with rate parameters obtained from numerical fitting procedures. The hexamerization kinetics show that the tetrameric intermediate transiently accumulates, forming rapidly at early time points and then decaying at a slower rate to generate the hexamer. The association of assembled ClpA hexamers with the ClpP core cylinder displays cooperativity, supporting the coexistence of interchanging ClpP conformations with different affinities for ClpA.

Chaperone−protease complexes are multisubunit assemblies that degrade protein substrates in all kingdoms of life (*1*, *2*). They have a two-component overall architecture consisting of a proteolytic cylinder lined with protease active sites and a ring-shaped chaperone complex. The shared architecture underlies a common mechanism of action. The chaperone rings bind to the ends of the proteolytic cylinder, acting as "entry guards", and they represent the site of recognition for potential protein substrates. After recognizing and binding substrates, the chaperones unfold and thread them into the proteolytic channel where they are then degraded into small peptides (*3*, *4*). Despite the common architecture and mode of action, different chaperone−protease complexes exist in eukaryotes, archaea, and eubacteria. Among the eubacterial chaperone−protease complexes, a very well-studied system is the ClpAP protease from *Escherichia coli* (*5*−*7*). ClpP forms the proteolytic core of the assembly consisting of two stacked heptameric rings. Lining the inside of the cavity are 14 serine protease active sites, one per subunit, arranged in two equatorial planes close to the center of the cavity (*8*). The regulatory ATPase ClpA forms hexameric rings, which has been shown by cryoelectron microscopy and analytical ultracentrifugation studies (*9*, *10*). ClpP on its own is able to hydrolyze small peptides (*11*), and ClpA can mediate ATP-dependent unfolding of substrate proteins in isolation (*12*). To carry out ATP-dependent protein degradation, ClpA hexamers have to bind to the ClpP cylinder, resulting in the fully assembled complex. In this complex, ClpA translocates substrate proteins into ClpP in a directional manner (*13*). ClpA and ClpP remain associated during the ATP-dependent degradation of protein substrates (*14*). Structurally, a ClpA monomer consists of three functional domains, an N-terminal helical domain involved in binding of adapter proteins and two AAA modules (termed D1 and D2) that are connected head to tail each containing Walker A and B nucleotide binding motifs (*15*). In the absence of nucleotide, ClpA has been shown to exist as a mixture of monomers and dimers (*10*). Only in the presence of ATP does ClpA assemble to its catalytically active hexameric form (*9*, *10*). This assembly is mediated by the first AAA module, and ClpA variants with mutations in the Walker A ATP-binding motif of this module are unable to form hexamers (*16*, *17*). The second AAA module forms the face of the hexamer that interacts with ClpP. ClpA variants with mutations in the Walker A motif of the second AAA module can still form hexamers but are unable to support substrate protein degradation in the presence of ClpP (*16*, *17*). While the oligomeric state of ClpA with nucleotide bound has been characterized, the mechanism and the accompanying kinetic parameters of ClpA assembly have not been elucidated. Both ClpA assembly and ClpAP complex formation were reported to occur on time scales requiring fast mixing techniques (*14*). Assembly of ClpA and association of ClpA hexamers with ClpP double rings have so far not been investigated in real time.

† This work was supported by the Swiss National Science Foundation (SNSF), the NCCR Structural Biology program of the SNSF, and a Roche graduate student fellowship to W.K.

* To whom correspondence should be addressed: Institute of Molecular Biology and Biophysics, ETH Zürich, Schafmattstrasse 20, CH-8093 Zürich, Switzerland. Phone: +41 44 633 3678. Fax: +41 44 633 1229. E-mail: eilika@mol.biol.ethz.ch.

10.1021/bi602616t CCC: $37.00 © 2007 American Chemical Society
Published on Web 05/04/2007

Here we study the nucleotide-induced oligomerization of ClpA into hexameric rings using intrinsic tryptophan fluorescence and light scattering to gain both dynamic and equilibrium information about this process. Combining the kinetic and equilibrium experimental data allows us to formulate a minimal mechanism for the ClpA oligomerization pathway that can serve as a model for the assembly of hexameric AAA+ proteins. We also study the assembly of the fully active complex from ClpA rings and ClpP double rings under pre-steady state conditions using rapid-kinetic methods.

EXPERIMENTAL PROCEDURES

Plasmids, Mutagenesis, and Protein Purification. ClpA, ClpP, and all protein variants were overexpressed in *E. coli* strain BL21(DE3) (Invitrogen) from plasmids harboring ClpA or ClpP under the T7 promoter. The ClpA variants ClpA(W229K), ClpA(W649Q/W689Y), and ClpA(W229K/W649Q/W689Y), which we later call ClpA(Wfree), as well as ClpP(E14W) were generated by using the QuikChange protocol (Stratagene). All constructs were verified by DNA sequencing. ClpA and all its variants were purified using ion exchange chromatography (SP Sepharose Fast Flow, Source30Q), ammonium sulfate precipitation, and size exclusion chromatography (High Load Superdex200). ClpPwt and ClpP(E14W) were purified using ion exchange chromatography (Q Sepharose Fast Flow, SP Sepharose Fast Flow). ClpAwt, ClpPwt, and all their variants were stored in 50 mM HEPES (pH 7.5), 0.3 M KCl, 15% (v/v) glycerol, and 2 mM EDTA. All chromatographic materials were purchased from Amersham Biosciences. Protein concentrations were determined spectroscopically by measuring the absorption at 280 nm.

ATPγS Purification. ATPγS was purchased from Roche and further purified by ion exchange chromatography (Resource Q) to remove residual ADP and AMP.

Fluorescence Spectra. Fluorescence emission spectra (λ_{ex} = 295 nm, and λ_{em} = 305−500 nm) were recorded in buffer R [50 mM HEPES (pH 7.5), 0.3 M KCl, 15% (v/v) glycerol, 0.5 mM EDTA, and 0.5 mM DTT] at 23 °C. A concentration of 6 μM ClpA (monomer) was used for ClpAwt and all its variants. ClpA assembly was induced by addition of 1 mM ATPγS and 20 mM $MgCl_2$, and emission spectra of hexameric ClpA were recorded after incubation for 10 min at 23 °C to ensure complete ClpA assembly. A fluorescence emission spectrum of 1.2 μM ClpA(Wfree) monomer with 0.1 μM $ClpP(E14W)_{14}$ was recorded in the absence of nucleotide and $MgCl_2$. ClpAP complex formation was then induced by addition of 1 mM ATPγS and 20 mM $MgCl_2$, giving a final $ClpA_6$:$ClpP_{14}$ ratio of 2:1. The fluorescence emission spectrum of assembled ClpAP was recorded after incubation for 10 min at 23 °C to allow complete complex formation. All fluorescence spectra were measured with a quantamaster (QM-7/2003) fluorimeter from Photon Technology International (PTI).

Titration of the ClpA Fluorescence Signal with Nucleotide. Nucleotide binding curves were obtained by incubating 0.6 or 6 μM ClpA monomer in buffer R with 20 mM $MgCl_2$ in the presence of increasing concentrations of ATPγS (from 0 to 1 mM) or ATP (from 0 to 5 mM) at 23 °C. At the higher ClpA concentration, 40 mM phosphocreatine (Sigma) and 25 units/mL of creatine phosphokinase (Sigma) were used to prevent ADP accumulation. The excitation wavelength was set to 295 nm, and the fluorescence signal at 340 nm was monitored. The relative change in fluorescence intensity given by $F_{rel} = F_{340nm}(ClpA_6)/F_{340nm}(ClpA)$ was normalized to the maximal intensity change measured at 6 μM ClpA.

Equilibrium Light Scattering Measurements. Oligomerization of ClpA was monitored by changes in 90° scattered light intensity as described by Singh et al. (*14*). ClpA monomer (6 μM) in buffer R and 20 mM $MgCl_2$ were mixed with increasing concentrations of ATPγS (from 0 to 1 mM) to induce ClpA hexamerization. All solutions were filtered through 0.2 μm syringe filters. Measurements were performed at 23 °C in a QM-7/2003 fluorimeter (PTI) with excitation and emission monochromators set to 360 nm. The relative change in scattered light intensity given by $S_{rel} = S_{360nm}(ClpA_6)/S_{360nm}(ClpA)$ was normalized against the maximal intensity change that was measured.

Continuous Spectrophotometric ATPase Assay. The ATPase activity was measured with a continuous spectrophotometric assay coupled to inorganic phosphate production using 7-methylinosine and the enzyme purine nucleoside phosphorylase (*18*).

For steady state measurements, the concentration of the ClpA monomer was 0.6 μM and the ATP concentration was varied from 0 to 5 mM. The reaction was carried out in buffer R and 20 mM $MgCl_2$ at 23 °C in a Cary UV−vis spectrophotometer (Varian).

For pre-steady state measurements, ClpA was rapidly mixed with 3 mM ATP in an SX.18MV stopped-flow instrument (Applied Photophysics). The change in ATP concentration in the beginning of the reaction is very small in comparison with the total concentration, so the velocity is given by

$$\frac{d[ATP]}{dt} = -k[ATP]_0[ClpA_6] \quad (1)$$

The delay for the appearance of active ClpA complex due to assembly can be approximated by a single exponential:

$$[ClpA_6] = [ClpA_6]_{tot}(1 - e^{-k_{delay}t}) \quad (2)$$

Combining eqs 1 and 2 and integration lead to the change in ATP concentration with time:

$$[ATP](t) = [ATP]_0\left[1 + [ClpA_6]_{tot}\frac{k}{k_{delay}}(1 - e^{-k_{delay}t} - k_{delay}t)\right] \quad (3)$$

This equation was fitted to the data. A constant d[ATP]/dt (in micromolar per second) indicates the steady state phase.

Rapid-Kinetic Analysis of ClpA Hexamerization and ClpAP Complex Formation. All stopped-flow experiments were carried out in an SX.18MV stopped-flow instrument from Applied Photophysics. The excitation wavelength was set to 295 nm, and the fluorescence intensity was detected at 340 nm. The scattered light intensity at 360 nm was recorded at a 90° angle. Oligomerization of ClpA was monitored after rapid mixing of ClpA with 1 mM ATPγS and 20 mM $MgCl_2$ in buffer R at 23 °C. The change in fluorescence intensity was measured at 0.6, 1.2, 2.4, 3.6, 6, and 12 μM ClpA

monomer. The increase in scattered light intensity was measured at 0.6, 1.2, 2.4, and 3.6 μM ClpA monomer. The change in tryptophan fluorescence intensity due to binding of ClpA(Wfree)$_6$ to ClpP(E14W)$_{14}$ was measured after rapid mixing of 0.1 μM ClpP(E14W)$_{14}$ with ClpA(Wfree) hexamer preassembled in buffer R with 1 mM ATPγS and 20 mM $MgCl_2$. Different ClpA(Wfree)$_6$ concentrations were used (0.25, 0.5, 0.75, 1, 1.5, and 2 μM).

Analytical Gel Filtration. ClpA (20 μL, 18 μM monomer) was applied on a Superose6PC (2.4 mL) gel filtration column (Amersham Biosciences). The column was equilibrated in buffer R with 1 mM ATPγS and 20 mM $MgCl_2$ where indicated. Absorbance was monitored at 227 nm. All experiments were performed at 23 °C.

Electron Microscopy. To confirm the integrity of the ClpAP complex composed of ClpA(Wfree) and ClpP-(E14W), we recorded negative stain electron microscopy images using conditions previously established by Kessel et al. (*9*). Specimens for electron microscopy were prepared by applying 20 μL aliquots of 30 nM ClpAPA complex in 50 mM Tris-HCl (pH 7.5), 0.2 M KCl, 20 mM $MgCl_2$, 10% (v/v) glycerol, and 1 mM ATPγS on freshly hydrophilized carbon-coated 400 mesh copper grids (Pelco) for 10 s, after which excess buffer was blotted off with filter paper. The specimens were washed two times with 20 μL of water. Twenty microliters of a 1% (w/v) uranyl acetate aqueous solution was applied to the grids; excess stain was blotted off, and the grids were allowed to dry. Specimens were viewed in a Zeiss Leo 912 transmission electron microscope operating at 120 kV at a magnification of 31500×.

Numerical Modeling and Fitting of Kinetic Data. All numerical procedures are described in the Supporting Information.

RESULTS

The Intrinsic Fluorescence Change of ClpA upon ATP-Induced Complex Formation Is Due to a Trp Residue in the First AAA Module. In the absence of nucleotide, ClpA exists in an unassembled state consisting of a mixture of ClpA monomers and dimers (*10*). Upon addition of ATP or the nonhydrolyzable analogue ATPγS, ClpA (subunit, 84 000 Da) assembles into hexameric rings with a molecular mass of 504 000 Da (*10*). The ClpA monomer contains three native tryptophan residues, one located in the first AAA module and the other two located in the second AAA module. We measured the intrinsic tryptophan fluorescence intensity of ClpA in the unassembled, nucleotide-free state and in the nucleotide-bound hexameric state. Upon addition of saturating amounts of ATPγS in the presence of $MgCl_2$, the intrinsic fluorescence intensity of wild-type ClpA increases by 39% (Figure 1a). To identify the tryptophan residue responsible for the signal change, we recorded fluorescence spectra of ClpAwt and two ClpA variants, one lacking the tryptophan in the D1 domain (W229K) and one lacking the two tryptophans in the D2 domain (W649Q/W689Y), in the absence and presence of ATPγS. Both variants were first tested for proper assembly into the hexameric form using analytical gel filtration in the presence of nucleotide. They both eluted at the same position as assembled ClpAwt (data not shown). The fluorescence intensity of ClpA(W649Q/W689Y) doubles upon addition of ATPγS and Mg^{2+} (Figure 1b), while no change can be detected for ClpA(W229K) (Figure 1c), as expected if Trp229 in the D1 domain (Figure 2) generates the entire signal change without contributions from either Trp649 or Trp689 in the D2 domain. When ATP was used in place of the nonhydrolyzable analogue, we obtained almost identical changes in the fluorescence intensities of wild-type ClpA and the two variants (data not shown). Since the signal change is seen with both ATP and its nonhydrolyzable analogue, the intensity changes cannot be due to a process driven by ATP hydrolysis but are caused by an event coupled to ATP binding.

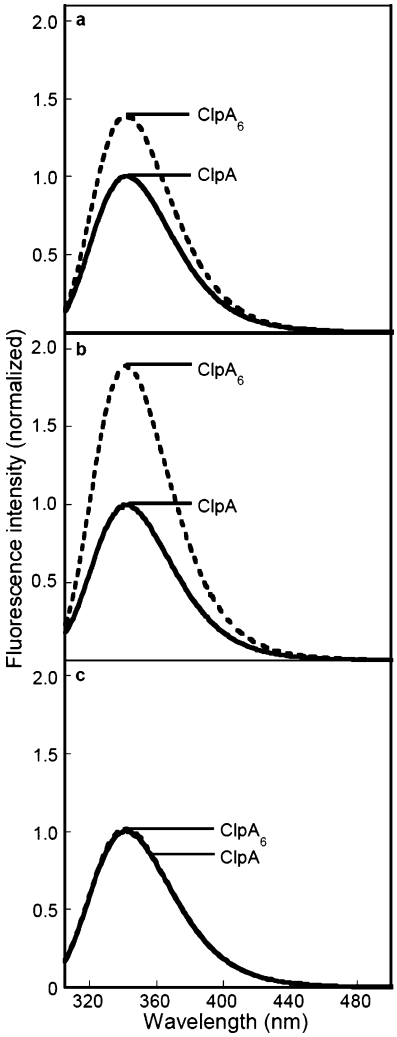

FIGURE 1: Trp229 reports on assembly of ClpA. Tryptophan fluorescence emission spectra of unassembled (solid line) and hexamerized (dashed line) ClpA were recorded. ClpA (a) and ClpA-(W649Q/W689Y) (b) show an increase in fluorescence upon hexamerization, whereas for ClpA(W229K) (c), no such increase can be detected. The hexamerization was induced by addition of ATPγS and Mg^{2+}.

The Fluorescence Signal Correlates with ATPase Activity and the Amount of Hexamer. The dependence of the intrinsic fluorescence of ClpA on nucleotide binding was used to obtain a binding curve for binding of ATP and ATPγS to ClpA. At the same time, the binding of nucleotide induces oligomerization of ClpA, and therefore, the binding titrations are likely to depend on the ClpA concentration. We thus measured the increase in the fluorescence intensity upon addition of increasing amounts of ATPγS (or ATP) at two different ClpA concentrations, yielding two binding curves

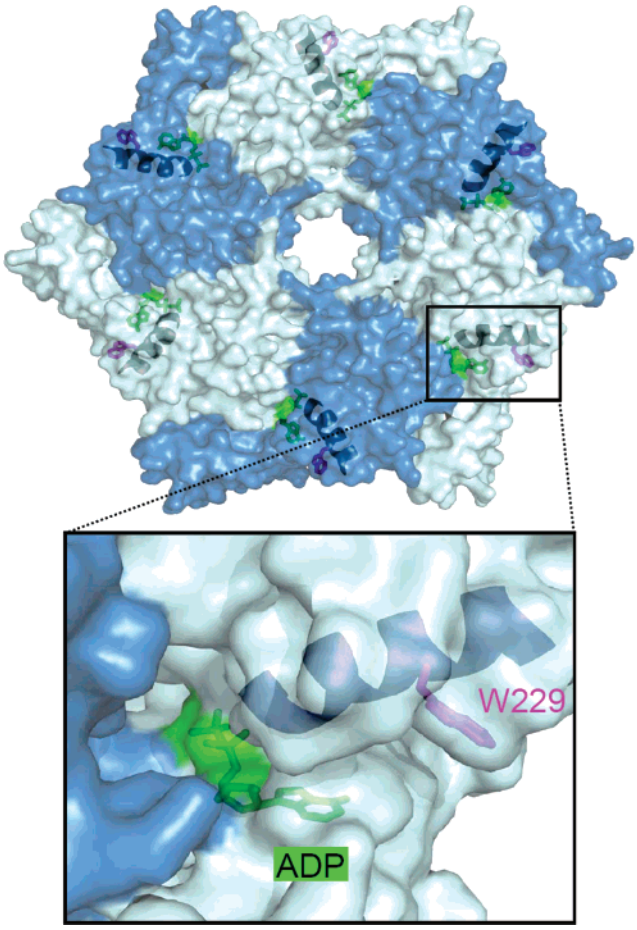

FIGURE 2: Location of Trp229 in a hexameric model of ClpA. Top view of a ClpA hexamer model with monomers colored alternatingly light and dark blue. Trp229 (magenta) is located at the end of a helix (ribbon) close to the Walker A motif where ADP (green) is bound. Trp229 lies on the periphery of the chaperone ring away from the subunit−subunit interface, which can be seen in the close-up view. The hexameric model of ClpA was built using the NSF and HslU hexamers as templates (*15*).

(Figure 3). The titration curves with ATPγS both display mildly sigmoidal behavior with different apparent affinities at the two concentrations. The concentration of nucleotide necessary to obtain half of the maximal signal change ($K_{1/2}$) is 60 μM when 6 μM ClpA (monomer) is used and more than twice as high (150 μM) when only 0.6 μM ClpA is used. The titration curves obtained with ATP display very similar behavior, but with higher $K_{1/2}$ values. At the higher ClpA concentration, the $K_{1/2}$ is 100 μM, and at the lower ClpA concentration, the $K_{1/2}$ is 460 μM.

As binding of nucleotide induces oligomerization of ClpA, it is reasonable to assume that the change in the fluorescence signal coming from Trp229 is due to hexamerization of ClpA. To test if, indeed, the tryptophan signal correlates with the amount of hexamer present, light scattering measurements were carried out. Formation of the ClpA hexamer leads to an increase in scattered light intensity that goes up linearly with the amount of complex formed for the chosen concentration range (data not shown). To compare the light scattering increase with the increase in fluorescence intensity, we measured the light scattering intensity of 6 μM ClpA (monomer) at increasing concentrations of ATPγS. After normalization of the data, the intensity changes in the scattered light (Figure 3a, red circles) overlay very well with the titration curve obtained by measuring the tryptophan fluorescence changes (Figure 3a, gray squares). Thus, the tryptophan signal reports directly on the amount of ClpA hexamer present at each concentration of nucleotide.

To test whether the fluorescence signal increase correlates not only with the assembly state but also with the activity displayed by the chaperone, we recorded the dependence of the ATPase activity on the ATP concentration for the lower ClpA concentration (0.6 μM monomer). The maximal activity (V_{max} = 590 ATP/ClpA$_6$ per min) was reached at ~3 mM ATP where according to fluorescence titration data ClpA is fully assembled. The normalized fluorescence intensity changes overlay very well with the normalized ATPase activity (Figure 3b, red rhombs).

To confirm that ClpA exhibits ATPase activity exclusively in the hexameric state, we compared the ATPase activity with the increase in fluorescence intensity upon hexamer formation (Figure 4). At a concentration of 0.12 μM ClpA monomer, the ATP-induced hexamerization and the accompanying ATPase activity were measured. Both types of measurements were carried out in a stopped-flow device to allow observation of the early time points of the reactions. For the ATPase activity time course, the first derivative was calculated to determine the time point at which the derivative became constant (this is equivalent to reaching the steady state). We found that ClpA achieves the steady state in ATPase hydrolysis at the same time as the tryptophan fluorescence reaches its maximal value (in Figure 4, compare the fluorescence time course with the derivative of the ATPase activity time course).

ClpA Hexamerization Proceeds through a Tetrameric Intermediate. To learn more about the assembly pathway, we investigated the kinetics of ClpA hexamerization following the tryptophan fluorescence signal at 340 nm (λ_{ex} = 295 nm) in a fluorescence stopped-flow device. To rule out additional components to the time courses due to ATP hydrolysis, the nonhydrolyzable ATP analogue ATPγS was used in these experiments. First, varying amounts of ClpA were rapidly mixed with saturating amounts of ATPγS and $MgCl_2$ to start the assembly reaction. The overall assembly process depends on the ClpA concentration and takes ~5 min to complete at the lowest concentration (0.1 μM ClpA$_6$), while at the highest concentration (2 μM ClpA$_6$), the reaction is over in ~1 min (Figure 5a). The time courses exhibit a fast phase with a very small amplitude followed by a slower phase likely representing the actual appearance of the hexamer. The first fast phase could correspond to formation of an assembly intermediate on the assembly pathway. While the ATPase activity is stringently dependent on the presence of Mg^{2+} ions, ATP can bind to ClpA even in the absence of Mg^{2+} ions, as a fluorescently labeled ATP analogue (TNP-ATP) that reports on nucleotide binding shows a signal change under these conditions (data not shown). We tested the fluorescence intensity change in the presence of ATPγS but without Mg^{2+} ions by rapidly mixing ClpA with ATPγS in the stopped-flow device. This revealed a fast signal change with a very small amplitude (only ~3.5% vs the 39% observed when Mg^{2+} ions are also present) similar to the first fast phase observed in the presence of Mg^{2+} ions. This could mean that under these conditions the assembly is arrested at the intermediate state on the pathway. To test this possibility and to obtain a more direct measure of the

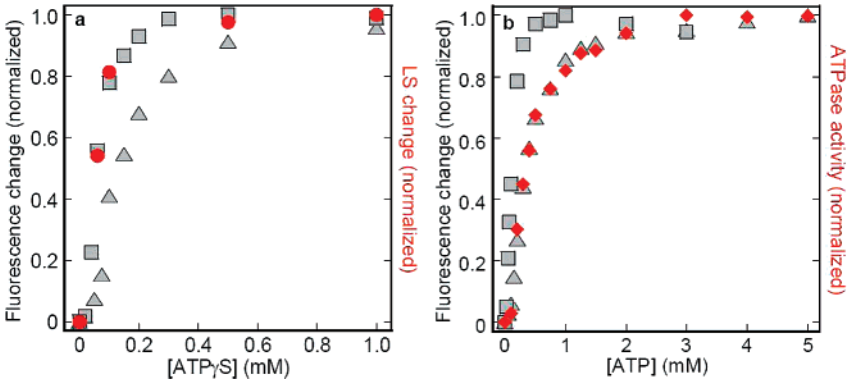

FIGURE 3: The fluorescence signal correlates with hexamerization state and ATPase activity. The change in fluorescence intensity upon hexamerization of 6 (squares) or 0.6 μM (triangles) ClpA monomer was measured. ClpA assembly was induced by addition of increasing concentrations of ATPγS (a) or ATP (b). To reach half of the final signal change, 150 μM ATPγS and 460 μM ATP are required for 0.6 μM ClpA monomer, whereas only 60 μM ATPγS and 100 μM ATP are sufficient for 6 μM ClpA. In addition, the assembly state of ClpA was monitored by light scattering (LS, red circles) at the higher ClpA concentration (a). The ATPase activity (red rhombs) was measured at the lower ClpA concentration (b), yielding a turnover number of 590 ATP/ClpA$_6$ per minute.

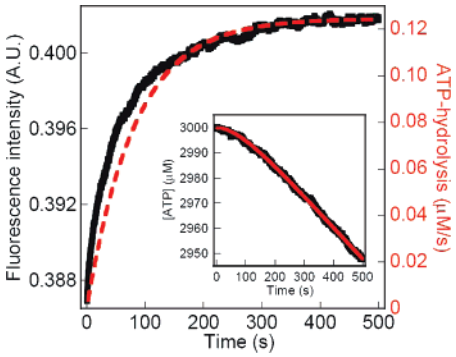

FIGURE 4: The maximal rate of hydrolysis is reached after ClpA assembly has been completed. Hexamerization of ClpA, followed by Trp fluorescence (black trace), and ATP hydrolysis (inset, black trace) were assessed after rapid mixing of 0.12 μM ClpA monomer with 3 mM ATP. ATP hydrolysis data were fitted to eq 3 (inset, red trace; see Experimental Procedures). The first derivative of the analytical fit (red dashed trace) gives the rate of ATP hydrolysis and shows that a constant ATPase activity is coinciding with the completion of ClpA hexamerization.

assembly state, we followed the assembly kinetics by stopped-flow light scattering measurements in the presence of ATPγS and $MgCl_2$ (Figure 5b). As in the fluorescence stopped-flow measurements, we started with the monomer−dimer equilibrium present with nucleotide-free ClpA. Upon rapidly mixing the sample with ATPγS and Mg^{2+} ions, we observed an increase in the light scattering intensity that clearly shows two stages: a first fast stage yielding a light scattering signal with a magnitude roughly two-thirds of that of the final signal and a slower second stage forming the hexameric ring structure. We also carried out two variations of the scattered light intensity stopped-flow experiment. In one case, we measured time courses upon mixing ClpA with ATPγS alone, generating the assembly intermediate, and in the other case, we followed the formation of hexamers from this intermediate state by rapidly mixing an equilibrated solution of ClpA and ATPγS with Mg^{2+} ions (Figure 6a). When mixing the sample with ATPγS in the absence of Mg^{2+} ions, we saw a rapid increase in the light scattering signal to a level corresponding to roughly two-thirds of the signal obtained with ATPγS and Mg^{2+} ions. This strongly suggests a tetrameric intermediate that accumulates under these conditions, since at a constant total weight per volume concentration of ClpA the change in the light scattering signal must be due entirely to a change in the assembly state. A population of tetramers should exhibit approximately two-thirds of the signal of a population of hexamers. Upon addition of Mg^{2+} ions, a slower increase in scattered light intensity corresponding to hexamer formation is observed. Figure 6b shows analytical gel filtration runs with ClpA performed at room temperature in the presence or absence of nucleotide and Mg^{2+} ions. Gel filtration runs of ClpA without nucleotide show an elution peak corresponding to the monomer/dimer mixture of unassembled ClpA (M/D). If the run is carried out in the presence of ATPγS and $MgCl_2$, the whole population elutes in a somewhat broader peak at an earlier elution volume corresponding to the hexameric ClpA assembly (H). Gel filtration runs in ATPγS but without Mg^{2+} ions show a single peak eluting at a position between where the monomer/dimer or hexamer elution peaks would be expected. This species likely corresponds to the tetrameric assembly intermediate (T) expected from the light scattering measurements. This peak is somewhat asymmetric, showing a tail extending out to the position where the monomer/dimer mixture would elute. This gives a hint that the tetramer is kinetically not very stable, and some complexes dissociate during the gel filtration run. A ClpA variant that assembles into hexamers much more slowly than the wild type exhibits at early time points in the assembly reaction a peak in gel filtration analysis eluting exactly at the position we observe for the wild type in ATPγS without $MgCl_2$. This peak then decays at later time points while the hexamer peak appears (data not shown). For the wild-type ClpA assembly, this intermediate is too transient to be detected via gel filtration analysis.

The oligomerization of ClpA is dependent on temperature and salt concentration. Fluorescence and scattered light intensity time courses were recorded after stopped-flow mixing of a ClpA solution with ATPγS and Mg^{2+} ions at three different temperatures (10, 23, and 35 °C) and three different salt concentrations (0.15, 0.3, and 0.6 M KCl) (see the Supporting Information).

An Engineered Trp Residue on the ClpP Double-Ring Surface Reports on Association with ClpA Hexamers. Assembled ClpA chaperone rings bind to both ends of the ClpP double ring to form the proteolytically active ClpAP

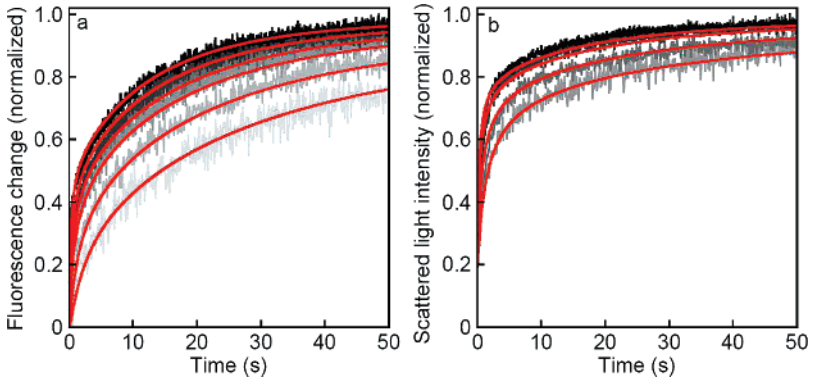

FIGURE 5: The ClpA hexamerization rate depends on the ClpA concentration. The tryptophan fluorescence change (a) and the increase in scattered light intensity (b) were monitored after rapid mixing of ClpA with ATPγS and Mg^{2+}. The time course of ClpA assembly was probed at ClpA monomer concentrations ranging from 0.6 to 12 μM (0.6, 1.2, 2.4, 3.6, 6, and 12 μM) for the fluorescence measurements and from 0.6 to 3.6 μM (0.6, 1.2, 2.4, and 3.6 μM) for the light scattering measurements. The increasing ClpA concentrations are indicated by a gray to black gradient. The time courses were fitted numerically (red traces) to a hexamerization pathway proposed in the discussion using the Berkeley Madonna software.

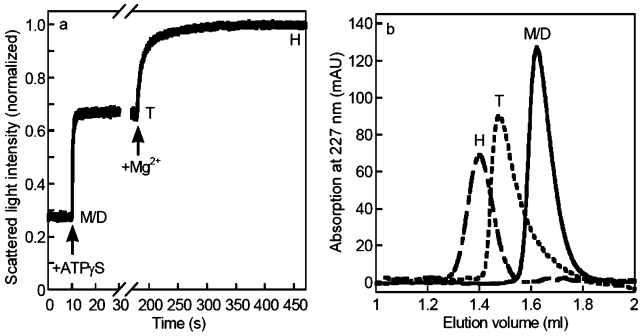

FIGURE 6: The tetrameric assembly intermediate accumulates in the presence of ATPγS without Mg^{2+}. (a) The increase in scattered light intensity was monitored after rapid mixing of ClpA monomer (M/D, 3.6 μM) with ATPγS in the absence of Mg^{2+}, yielding a ClpA assembly intermediate (T). Subsequently, a solution containing the assembly intermediate (ClpA incubated with ATPγS without Mg^{2+} for 180 s) was rapidly mixed with Mg^{2+}, resulting in a further increase in scattered light intensity due to the hexamerization of ClpA (H). The assembly intermediate holds two-thirds of the final scattered light intensity of the hexamer, suggesting a tetrameric intermediate. (b) The oligomeric state of ClpA was analyzed using a Superose6PC gel filtration column. ClpA runs as a mixture of monomer and dimer (solid line, M/D) in the absence of nucleotide. The tetrameric state (dashed line, T) of ClpA is formed in the presence of ATPγS. When Mg^{2+} and ATPγS are both present, ClpA forms the fully assembled hexamer (interrupted line, H).

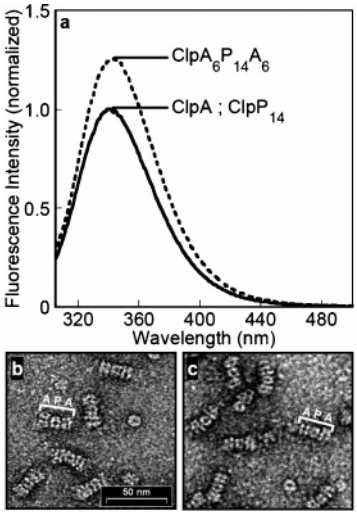

FIGURE 7: ClpA−ClpP interaction can be followed by fluorescence intensity changes. (a) The tryptophan fluorescence intensity change upon binding of ClpA(Wfree) to ClpP(E14W) was measured. The spectra of ClpP(E14W) together with ClpA(Wfree) were obtained in the absence (solid line) or presence (dashed line) of ATPγS and Mg^{2+}. ClpA refers to the unassembled monomer/dimer mixture, $ClpP_{14}$ to the ClpP core cylinder, and $ClpA_6P_{14}A_6$ to the fully assembled ClpAP complex with two ClpA hexamers bound to each end of the ClpP 14-membered double ring. Negative stain electron microscopy images of the wild-type ClpAP complex (b) and the ClpP(E14W)−ClpA(Wfree) complex (c) at 31500× magnification demonstrate that ClpA−ClpP interaction is not perturbed due to the amino acid replacements in ClpA and ClpP.

chaperone−protease complex. The recently published X-ray structure of ClpP from *Streptococcus pneumoniae* revealed the existence of an N-terminal loop important for ClpAP or ClpXP complex formation protruding from the apical surface of ClpP (*19*). The authors also showed that a tryptophan residue placed in position 14 of this loop region exhibits fluorescence intensity changes upon complex formation with ClpX (*19*). To probe the association of ClpA hexamers with the ClpP core cylinder, we introduced a tryptophan into this position at the ClpP ring surface (E14W). To prevent fluorescence intensity changes arising from the three intrinsic tryptophan residues of ClpA that could interfere with the signal change upon association due to the engineered tryptophan residue, we produced a tryptophan-free ClpA variant. Size exclusion chromatography (data not shown) and electron microscopy (Figure 7b,c) verified that this variant assembles into hexamers and can form ClpAP complexes with ClpP(E14W) like ClpAwt with ClpPwt. Binding of the tryptophan-free ClpA variant to ClpP(E14W) was assayed by monitoring the fluorescence of Trp14 on the ClpP ring surface. An increase in the fluorescence intensity due to the engineered tryptophan of 25% was observed (Figure 7a).

Association of ClpA Hexamers with the ClpP Double Ring. The ClpA hexamer assembled in ATPγS is stable over several hours (data not shown). Preassembled ClpA hexamer can, therefore, be used to analyze the association of ClpA rings with ClpP double rings. We performed fluorescence stopped-flow measurements in which ATPγS-preassembled ClpA was rapidly mixed with ClpP. To probe the concentration dependence of the association kinetics, the concentration of ClpA hexamer was varied from 0.25 to 2 μM at a constant concentration of ClpP double ring of 0.1 μM. In this concentration range, binding of the ClpA hexamer to the

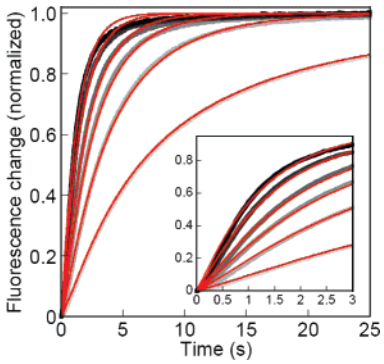

FIGURE 8: ClpAP assembly kinetics reveal positive cooperativity. The increase in tryptophan fluorescence intensity was measured after rapid mixing of 0.1 μM ClpP(E14W)$_{14}$ with 0.25−2 μM (0.25, 0.5, 0.75, 1, 1.5, and 2 μM) ClpA(Wfree)$_6$, preassembled in ATPγS and Mg^{2+}. Increasing ClpA concentrations are indicated by a gray to black gradient. The kinetic data were fitted to an assembly mechanism accounting for cooperativity according to an MWC model (red traces). The inset displays the first 3 s of the ClpAP assembly reaction.

ClpP 14-mer occurs in 10 and 100 s at the highest and lowest ClpA concentrations, respectively (Figure 8). To confirm that the fluorescence change reports on the process of ClpA and ClpP association, stopped-flow light scattering measurements were also carried out under the same conditions (data not shown). Both time courses overlay well on top of one another after normalization of the signals, arguing strongly that burial of the Trp residue on the surface of the ClpP ring upon association with the ClpA ring gives rise to the fluorescence signal change.

ClpA Hexamerization Precedes ClpAP Complex Formation. As demonstrated in Figure 4, ClpA exhibits ATPase activity only in the hexameric state. We tested whether ClpA in a nonassembled state (dimer or monomer) can interact with ClpP or whether formation of the hexamer is a prerequisite for association with ClpP. Rapid mixing of preassembled ClpA hexamers with ClpP results in a fast binding event of hexamers to the ClpP 14-mer (Figure 9a, black solid trace). However, if ClpA is not assembled prior to being mixed with ClpP, the association with ClpP is considerably slower (dashed trace). Comparison with the hexamerization time course at the same ClpA concentration (red trace) shows that the rate of ClpAP complex formation is clearly limited by the hexamerization process. In the absence of nucleotide, ClpA−ClpP association was entirely eliminated (interrupted trace). These results suggest that ClpA can only bind to the ClpP 14-mer in its assembled hexameric state. In addition, we can rule out the possibility that the ClpP 14-mer acts as a template for ClpA hexamerization, since ClpP does not accelerate ClpA hexamer formation (Figure 9b).

DISCUSSION

Chaperone−protease complexes are mechanochemical molecular machines that disassemble, unfold, and degrade proteins at the expense of energy. Like most molecular machines, they are composed of multiple subunits and need to assemble into a larger architecture to become biologically active. Chaperone−protease complexes have a cylindrical design that compartmentalizes their destructive activity away from the cytosol and regulates access of substrates to the degradation chamber. The *E. coli* ClpAP chaperone−protease complex consists of two types of subunits, the chaperone subunit ClpA and the proteolytic subunit ClpP. ClpP assembles spontaneously into a stable double-ring structure (*10*). In the absence of ATP, ClpA remains unassembled and inactive, while in the presence of nucleotide, it assembles into a hexameric ring structure. Hexameric ClpA rings associate with the ClpP core cylinder to form the fully active chaperone−protease complex.

Nature of the Intrinsic Fluorescence Change in ClpA upon Nucleotide-Induced Oligomerization. In an effort to assess ClpA hexamer assembly spectroscopically, we tested the properties of the intrinsic tryptophan fluorescence of ClpA in the assembled and unassembled state. The *E. coli* ClpA monomer contains three tryptophan residues, one located in the first AAA module and the other two located in the second AAA module. These tryptophans are conserved only across the very highly conserved enterobacterial members of the ClpA family and can be replaced without impairment of function. By substituting the tryptophans in AAA module 1 or 2, we could show that only the tryptophan in the first AAA domain contributes to the signal change. This signal change upon hexamer formation could be due to two events: either a change in solvent accessibility upon formation of the ClpA−ClpA interface in the hexamer or a change in interactions with neighboring polar groups accompanying a conformational change upon hexamer formation. In the modeled ClpA hexamer, Trp229 located in the first AAA module lies on the periphery of the chaperone ring away from the subunit−subunit interface and appears as solvent exposed as in the monomer (Figure 2). Trp229 is located opposite the α-helical subdomain of the first AAA module, ~10 Å from the closest residue in the helical domain. Furthermore, it is located only nine residues away on the same helix as Lys220 of the Walker A motif and is close to the loop region that makes contact with the adenine moiety of ATP. Given the presumably rather small changes in solvent accessibility and the location of Trp229 close to the α-helical domain, a conformational change is the most likely cause for the observed signal change. A large conformational change has, for example, been detected upon binding of ATP to p97 AAA ATPase by electron microscopy (*20*). As demonstrated by comparison of the fluorescence titration curves with light scattering and ATPase activity measurements, the signal change is directly connected to formation of the ATPase-active conformation of the ClpA hexamer. The assembly state and the assembly kinetics of ClpA are dependent both on the nucleotide and on the ClpA concentration, because ATP binding and oligomerization are coupled.

Hexamer Assembly Pathway. As a member of the AAA+ protein family, the assembled ClpA hexamer exhibits 6-fold rotational symmetry with the AAA modules aligned in a head-to-tail fashion. The assembly kinetics of such homohexamers are complex, and several assembly pathways are possible. Three different types of mechanisms can be primarily distinguished. The first is a mechanism involving the stepwise addition of monomers to a growing oligomer dimers, trimers, tetramers, and pentamers as intermediates. The second is a mechanism with the dimer as the building block and the third a mechanism based on a trimer as the building block. Our data argue strongly for a monomer−

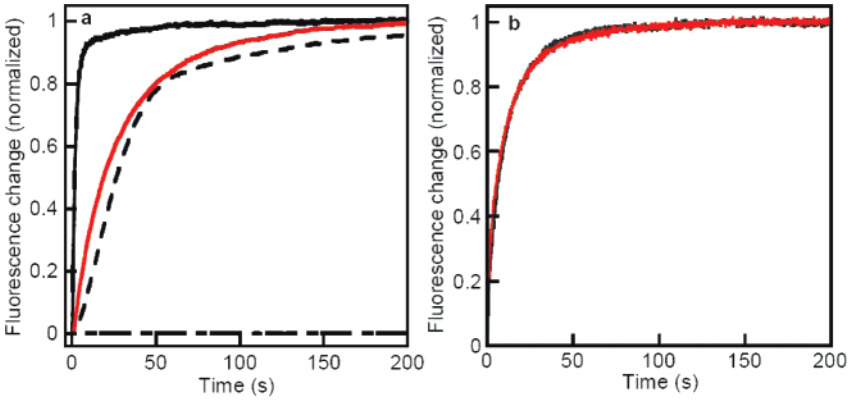

FIGURE 9: Hexamerization of ClpA precedes ClpAP complex formation and is not accelerated by ClpP. (a) ClpAP complex formation was monitored by the fluorescence intensity change after mixing of ClpP(E14W) with unassembled ClpA(Wfree) (dashed trace) or preassembled ClpA(Wfree) (black solid trace) in the presence of ATPγS and Mg^{2+}. In the absence of the nucleotide, no ClpAP complex formation was observed (interrupted trace). ClpAwt hexamerization (red solid trace), followed by Trp229 fluorescence, occurred on a time scale similar to that of ClpAP complex formation from unassembled ClpA and ClpP double rings. Concentrations were 0.1 μM ClpP double ring and 6 μM ClpA (monomer). (b) Hexamerization of ClpA (12 μM monomer) was assessed in the absence (red trace) and presence (black trace) of 1 μM ClpP 14-mer by following the fluorescence change of Trp229 in ClpA after rapid mixing with ATPγS and Mg^{2+}.

dimer−tetramer−hexamer pathway (MDTH pathway) as we observe a fast increase in the light scattering signal to a level corresponding to roughly two-thirds of the signal observed in fully assembled hexamers in the first stage of the reaction. Upon addition of nucleotide without Mg^{2+} ions, the assembly process is even arrested at this intermediate stage. In agreement with this interpretation, analytical gel filtration runs under these conditions show a peak eluting between the positions of hexamers and of the monomer/dimer mixture exactly at a position where the tetrameric species would be expected. The tetrameric assembly intermediate is further supported by the observation that for a ClpA variant with slowed overall assembly kinetics the intermediate converts to the hexamer slowly enough that it can be visualized by gel filtration (data not shown). For the wild-type protein, this intermediate is too transient to be detected via this method. On the basis of these observations and the fact that unassembled ClpA exists in a dimer−monomer equilibrium, a mechanism that proceeds through a tetrameric intermediate seems highly plausible. Furthermore, a pure annealing type of mechanism where monomer after monomer is added is not sustainable due to the many kinetic traps resulting from the dependence on a decreasing monomer pool. To overcome such traps, intermediates would have to exhibit low affinities for monomers, which on the other hand hamper efficient hexamer formation. Hexamer assembly through a dimer mechanism requires fewer assembly steps, and kinetic traps can more easily be avoided.

While the kinetics of hexamerization are too complex to be determined analytically, we generated a numerical model based on the MDTH pathway (Figure 10a). It is assumed that when the nucleotide-free ClpA monomer/dimer population is mixed with ATPγS and $MgCl_2$, nucleotide is rapidly bound and the reaction essentially starts with a ratio of monomers and dimers equal to the one before addition of nucleotide. However, with nucleotide bound, this ratio no longer corresponds to the equilibrium distribution, because the equilibrium constant between monomers and dimers in the nucleotide-bound state is strongly shifted toward dimers. The oligomerization reaction is initiated by this event, and the pathway follows a scheme in which monomers associate to form dimers, dimers associate with each other to form tetramers, and tetramers associate with dimers to reach the hexameric fully assembled state. The final step in the assembly pathway, the hexamerization, is followed by a very fast conformational change locking the hexamer into the active conformation. This fast conformational change upon hexamer formation is the cause of the observed change in the tryptophan fluorescence intensity. In the reaction scheme, the hexamerization step and the conformational change have been combined in a single step. The light scattering stopped-flow kinetic data obtained at different concentrations of ClpA report directly on the average molecular weight of the complexes present at any given time point. The stopped-flow time courses using the tryptophan fluorescence as a signal on the other hand report on the last step of the oligomerization scheme, the formation of the active hexamer conformation. The time courses obtained from both methods and for all the recorded ClpA concentrations were numerically fitted to the MDTH pathway model using the Berkeley Madonna software. Panels a and b of Figure 5 show the experimental curves together with the obtained fits. The differential equations used to generate the model as well as the equations formulated to give the fluorescence and light scattering time courses are given in the Supporting Information. The fit generates values for the forward and reverse rate parameters of all three oligomerization steps: the dimerization step (k_1 and k_{-1}), the tetramerization step (k_2 and k_{-2}), and the hexamerization step (k_3 and k_{-3}). The association constant for the initial equilibrium between monomers and dimers in the absence of nucleotide was previously determined by analytical ultracentrifugation by Maurizi et al. (*10*). It was, therefore, set as a fixed parameter in the final fitting procedure for calculation of the initial concentration of ClpA monomer and ClpA dimer. When the monomer/dimer mixture is mixed with nucleotide, the monomer−dimer equilibrium is strongly shifted toward an assembly competent form of the dimer, and the oligomerization is thus initiated. The bimolecular rate constants for the three oligomerization steps are not identical. The dimerization and hexamerization are one order of magnitude slower than the tetramerization step, leading to accumulation of the tetramer at early time points and slow decay of the tetramer to generate hexamer (Figure 11).

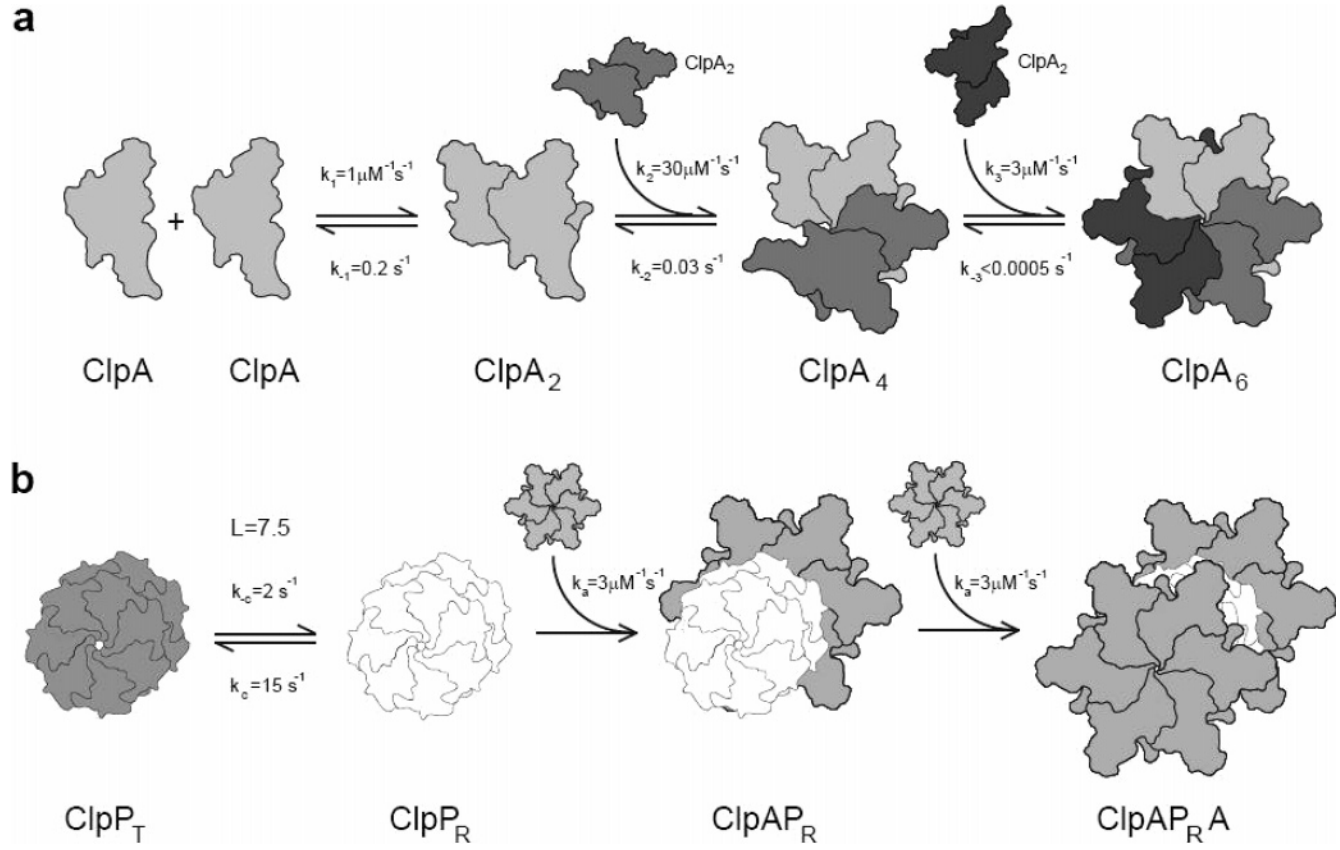

FIGURE 10: Model of the ClpA assembly pathway and ClpAP complex formation. (a) The ClpA monomer−dimer equilibrium is present in the absence of ATP and Mg^{2+}. When ATP and Mg^{2+} bind, the monomer−dimer equilibrium is defined by altered forward and reverse rate constants, k_1 and k_{-1}, respectively. A tetramer forms as a transient intermediate (k_2 and k_{-2}), which then binds another dimer to form the hexamer (k_3 and k_{-3}). (b) Binding of $ClpA_6$ to $ClpP_{14}$ occurs after the hexamerization process. The ClpP cylinder adopts two conformations that coexist in solution (P_R and P_T). The interconversion of both is described by the equilibrium constant L. In this model, only PR can associate with ClpA (k_a) while PT cannot. The indicated kinetic parameters were obtained by numerical fitting of the experimental data to the presented models.

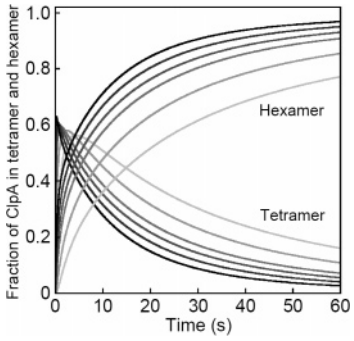

FIGURE 11: Berkeley Madonna simulation of ClpA hexamerization. The assembly process of ClpA was simulated using the rate constants obtained from the numerical fit. The increasing ClpA concentrations are indicated by a gray to black gradient. The ClpA tetramer is transiently formed and binds a ClpA dimer, giving the ClpA hexamer. The overall hexamerization process is completed after approximately 1 min at the highest ClpA concentration (2 μM $ClpA_6$). The *y*-axis shows the fraction of the total amount of ClpA monomers that is present in tetramers ($4[T]/[M]_{total}$) or hexamers ($6[H]/[M]_{total}$).

The association steps are sensitive to salt concentration, leading to a decrease in the amount of hexamer particularly at high salt concentrations. This suggests that the interfaces between the subunits involve salt-sensitive interactions. The formation of hexamer is significantly slowed at lower temperatures (10 °C), and it appears that particularly the second, slower stage of the assembly reaction, the decay of tetramers to form hexamers, is affected.

Association of ClpA Rings with the ClpP Proteolytic Cylinder. To build the active chaperone−protease complex, the nucleotide binding-induced ClpA hexamers have to associate with the ClpP double ring. As demonstrated by comparison of the hexamerization time courses with the time traces for ClpA−ClpP association, ClpA hexamerization is kinetically limiting. This indicates that hexamerization is a prerequisite for association with ClpP. ClpA rings that have assembled into hexamers in the presence of ATPγS and $MgCl_2$ associate with the ClpP double ring with kinetics that are highly dependent on the ClpA hexamer concentration (Figure 8). The individual fluorescence time courses display at the early time points a mildly sigmoidal shape indicative of cooperative behavior. The very elegant yet simple model for cooperativity proposed in 1965 by Monod, Wyman, and Changeux (MWC model) can be applied to account for the behavior we observe for ClpA association to ClpP (*21*). The ClpP cylinder is proposed to adopt two conformations that coexist in solution, termed P_R and P_T, the interconversion of which is described by the equilibrium constant L with the forward and reverse rate constants k_c and k_{-c}, respectively. The two conformations should display markedly different affinities for the ClpA hexamer. Interestingly, the high-resolution X-ray structure of ClpP shows alternative conformations for a loop in the mature N-terminus located

at the ClpP apical surface (*22*). In ClpP from *S. pneumoniae* this loop has been shown to play a role in the interaction with ClpA or ClpX rings (*19*). In our model, we assume for further simplification that only P_R can associate with ClpA while P_T cannot. Association of the first ClpA hexameric ring with the $ClpP_R$ double ring redistributes the ratio of ClpP ring faces in favor of the R conformation, giving rise to the observed cooperativity. As the apparent dissociation constant has previously been shown to be approximately 4 nM (*10*), the dissociation rate constants must be very small and for the purpose of simplification were neglected. Numerical fitting of the experimental curves to this model yields an equilibrium constant L of 7.5 with a k_c of 15 s^{-1} and a k_{-c} of 2 s^{-1}. The microscopic bimolecular association rate constant (k_a) for binding of the ClpA hexamer to ClpP double rings is 3 μM^{-1} s^{-1}.

An average-sized *E. coli* cell contains ~50−150 copies of ClpA hexameric rings depending on the growth conditions (*23*). Using an average total cell volume for *E. coli* of 10^{-15} L, this results in an in vivo concentration range for the ClpA hexamer of 0.05−0.5 μM. At these concentrations, the hexamer assembly process takes ~2 min. ClpP double-ring complexes are present at a density of ~100−300 copies per cell depending on growth conditions (*23*), resulting in a concentration range of 0.1−1 μM ClpP double rings. This means that association of ClpA hexamers with ClpP double rings should take ~1−2 min inside the cell. ClpA hexamerization and association with ClpP thus take place on very similar time scales.

Many AAA+ proteins must assemble into hexameric ring structures to be functional. Oligomerization can, therefore, also serve as a regulatory mechanism in controlling the activity of some AAA+ complexes. A recently described example of such control is present in the ClpC AAA+ protein of *Bacillus subtilis*. ClpC controls important steps of developmental processes in this organism, like competence and sporulation (*24*). It has now been shown that the oligomerization of ClpC is controlled by an adaptor protein, MecA, which binds to unassembled subunits, thus triggering the assembly reaction (*25*). The assembly mechanism of the ClpA hexamer could serve as a model for the assembly of other hexameric AAA+ proteins. Understanding the oligomerization pathway of AAA+ proteins forms a good basis for investigating regulation of assembly in this protein family.

ACKNOWLEDGMENT

We thank Stefan Pitsch for synthesizing 7-methylinosine used in the spectrophotometric ATPase assay and Arthur Horwich for providing the ClpA and ClpP overexpressing plasmids. We also thank Ulla Grauschopf, Michael Vetsch, and members of the Weber-Ban research group for critically reading the manuscript. Electron microscopy was performed at the Electron Microscopy Center of ETH Zürich (EMEZ).

SUPPORTING INFORMATION AVAILABLE

Numerical modeling and fitting procedures for ClpA hexamerization and ClpAP complex formation and oligomerization time traces at different temperatures and salt concentrations. This material is available free of charge via the Internet at http://pubs.acs.org.

REFERENCES

1. Lupas, A., Flanagan, J. M., Tamura, T., and Baumeister, W. (1997) Self-compartmentalizing proteases, *Trends Biochem. Sci. 22*, 399−404.
2. Suzuki, C. K., Rep, M., van Dijl, J. M., Suda, K., Grivell, L. A., and Schatz, G. (1997) ATP-dependent proteases that also chaperone protein biogenesis, *Trends Biochem. Sci. 22*, 118−123.
3. Gottesman, S. (1996) Proteases and their targets in *Escherichia coli*, *Annu. Rev. Genet. 30*, 465−506.
4. Sauer, R. T., Bolon, D. N., Burton, B. M., Burton, R. E., Flynn, J. M., Grant, R. A., Hersch, G. L., Joshi, S. A., Kenniston, J. A., Levchenko, I., Neher, S. B., Oakes, E. S., Siddiqui, S. M., Wah, D. A., and Baker, T. A. (2004) Sculpting the proteome with AAA-(+) proteases and disassembly machines, *Cell 119*, 9−18.
5. Hwang, B. J., Woo, K. M., Goldberg, A. L., and Chung, C. H. (1988) Protease Ti, a new ATP-dependent protease in *Escherichia coli*, contains protein-activated ATPase and proteolytic functions in distinct subunits, *J. Biol. Chem. 263*, 8727−8734.
6. Katayama-Fujimura, Y., Gottesman, S., and Maurizi, M. R. (1987) A multiple-component, ATP-dependent protease from *Escherichia coli*, *J. Biol. Chem. 262*, 4477−4485.
7. Katayama, Y., Gottesman, S., Pumphrey, J., Rudikoff, S., Clark, W. P., and Maurizi, M. R. (1988) The two-component, ATP-dependent Clp protease of *Escherichia coli*. Purification, cloning, and mutational analysis of the ATP-binding component, *J. Biol. Chem. 263*, 15226−15236.
8. Wang, J., Hartling, J. A., and Flanagan, J. M. (1997) The structure of ClpP at 2.3 Å resolution suggests a model for ATP-dependent proteolysis, *Cell 91*, 447−456.
9. Kessel, M., Maurizi, M. R., Kim, B., Kocsis, E., Trus, B. L., Singh, S. K., and Steven, A. C. (1995) Homology in structural organization between *E. coli* ClpAP protease and the eukaryotic 26 S proteasome, *J. Mol. Biol. 250*, 587−594.
10. Maurizi, M. R., Singh, S. K., Thompson, M. W., Kessel, M., and Ginsburg, A. (1998) Molecular properties of ClpAP protease of *Escherichia coli*: ATP-dependent association of ClpA and clpP, *Biochemistry 37*, 7778−7786.
11. Woo, K. M., Chung, W. J., Ha, D. B., Goldberg, A. L., and Chung, C. H. (1989) Protease Ti from *Escherichia coli* requires ATP hydrolysis for protein breakdown but not for hydrolysis of small peptides, *J. Biol. Chem. 264*, 2088−2091.
12. Weber-Ban, E. U., Reid, B. G., Miranker, A. D., and Horwich, A. L. (1999) Global unfolding of a substrate protein by the Hsp100 chaperone ClpA, *Nature 401*, 90−93.
13. Reid, B. G., Fenton, W. A., Horwich, A. L., and Weber-Ban, E. U. (2001) ClpA mediates directional translocation of substrate proteins into the ClpP protease, *Proc. Natl. Acad. Sci. U.S.A. 98*, 3768−3772.
14. Singh, S. K., Guo, F., and Maurizi, M. R. (1999) ClpA and ClpP remain associated during multiple rounds of ATP-dependent protein degradation by ClpAP protease, *Biochemistry 38*, 14906−14915.
15. Guo, F., Maurizi, M. R., Esser, L., and Xia, D. (2002) Crystal structure of ClpA, an Hsp100 chaperone and regulator of ClpAP protease, *J. Biol. Chem. 277*, 46743−46752.
16. Seol, J. H., Baek, S. H., Kang, M. S., Ha, D. B., and Chung, C. H. (1995) Distinctive roles of the two ATP-binding sites in ClpA, the ATPase component of protease Ti in *Escherichia coli*, *J. Biol. Chem. 270*, 8087−8092.
17. Singh, S. K., and Maurizi, M. R. (1994) Mutational analysis demonstrates different functional roles for the two ATP-binding sites in ClpAP protease from *Escherichia coli*, *J. Biol. Chem. 269*, 29537−29545.
18. Rieger, C. E., Lee, J., and Turnbull, J. L. (1997) A continuous spectrophotometric assay for aspartate transcarbamylase and ATPases, *Anal. Biochem. 246*, 86−95.
19. Gribun, A., Kimber, M. S., Ching, R., Sprangers, R., Fiebig, K. M., and Houry, W. A. (2005) The ClpP double-ring tetradecameric protease exhibits plastic ring-ring interactions, and the N-termini of its subunits form flexible loops that are essential for ClpXP and ClpAP complex formation, *J. Biol. Chem. 280*, 16185−16196.
20. Rouiller, I., Butel, V. M., Latterich, M., Milligan, R. A., and Wilson-Kubalek, E. M. (2000) A major conformational change in p97 AAA ATPase upon ATP binding, *Mol. Cell 6*, 1485−1490.

21. Monod, J., Wyman, J., and Changeux, J. P. (1965) On the Nature of Allosteric Transitions: A Plausible Model, *J. Mol. Biol. 12*, 88−118.
22. Bewley, M. C., Graziano, V., Griffin, K., and Flanagan, J. M. (2006) The asymmetry in the mature amino-terminus of ClpP facilitates a local symmetry match in ClpAP and ClpXP complexes, *J. Struct. Biol. 153*, 113−128.
23. Farrell, C. M., Grossman, A. D., and Sauer, R. T. (2005) Cytoplasmic degradation of ssrA-tagged proteins, *Mol. Microbiol. 57*, 1750−1761.
24. Turgay, K., Persuh, M., Hahn, J., and Dubnau, D. (2001) Roles of the two ClpC ATP binding sites in the regulation of competence and the stress response, *Mol. Microbiol. 42*, 717−727.
25. Kirstein, J., Schlothauer, T., Dougan, D. A., Lilie, H., Tischendorf, G., Mogk, A., Bukau, B., and Turgay, K. (2006) Adaptor protein controlled oligomerization activates the AAA+ protein ClpC, *EMBO J. 25*, 1481−1491.

BI602616T